

Phase Diagram of a Lipid Monolayer on the Surface of Water

B. Lin, M. C. Shih, and T. M. Bohanon

Department of Physics and Astronomy, Northwestern University, Evanston, Illinois 60208

G. E. Ice

Metals and Ceramics Division, Oak Ridge National Laboratory, Oak Ridge, Tennessee 37830

P. Dutta

Department of Physics and Astronomy, Northwestern University, Evanston, Illinois 60208

(Received 7 September 1989)

The monolayer isotherms of heneicosanoic acid show a variety of features in the range 1–8°C; such features are often assumed to be solid-fluid or fluid-fluid transitions. Using x-ray diffraction (and searching for in-plane and off-plane peaks) we find (a) two distinct distorted-hexagonal (DH) solids at high pressures, both with essentially vertical chains; (b) two distinct tilted-DH solids at intermediate pressures; and (c) an expanded solid at the lowest pressures. All “plateaus” in these isotherms are in-plane structural transitions; all “kinks” are solid-solid tilting transitions.

PACS numbers: 68.55.Nq, 61.65.+d

The isotherms of organic monolayers at the air-water interface (Langmuir films) frequently show features suggesting phase transitions;¹ Langmuir's 1917 paper² showing the first discontinuous isotherms led to an explosion of interest in these systems that continues to this day. However, it is only since 1987 that direct structural information has become available.^{3–8} During the intervening seventy years, although in the absence of microscopic data there has naturally been no consensus regarding the structures of these phases, speculative labels such as “liquid expanded,” “liquid condensed,” etc.,⁹ have gained currency and are now widely used.

We will describe in this paper our x-ray-diffraction studies of Langmuir films of heneicosanoic acid between 1.0 and 8.0°C (a region in which the isotherms show a variety of features and trends; see Fig. 1). These experiments were performed at beam line X-14 of the National Synchrotron Light Source. The basic principles of this experiment have been described in Ref. 5; we have added a new hermetically sealed trough with wider windows, and we can now move our detector away from the plane of the monolayer. In other words, we are now able to locate off-plane diffraction peaks. Monolayer temperature can be controlled to 0.1°C by circulating water through channels below the trough and in the lid. In the experiments to be described, a helium atmosphere was maintained in the enclosure; this reduced the scattering background and also eliminated the time-dependent effects seen otherwise¹⁰ (implying that these effects were due to radiation-induced oxidation).

The x-ray beam was monochromatized to $E = 8.5$ keV; the vertical angle of incidence on the monolayer was $\sim 1.7 \times 10^{-3}$ rad (the critical angle for total reflection is $\sim 2.5 \times 10^{-3}$ rad). Two Soller slits—one vertical and one horizontal—were positioned in front of the detector to define the beam. The resolution for K_{xy} was ~ 0.01

\AA^{-1} FWHM; all diffraction peaks reported in this paper were resolution limited in the horizontal plane, implying correlation lengths larger than ~ 500 \AA . Since the molecules are not point particles, the diffraction peaks are not literally “rods”; however, the peaks are intrinsically broader vertically than horizontally. In order to achieve reasonable count rates, we used a vertical resolution of ~ 0.2 \AA^{-1} FWHM, which is roughly equal to the intrinsic vertical width.

Heneicosanoic acid is a simple single-chain lipid, $\text{CH}_3(\text{CH}_2)_{19}\text{COOH}$. It is longer than some of the more familiar lipids (e.g., stearic acid), and so is less soluble and more stable in monolayer form. Isotherms were

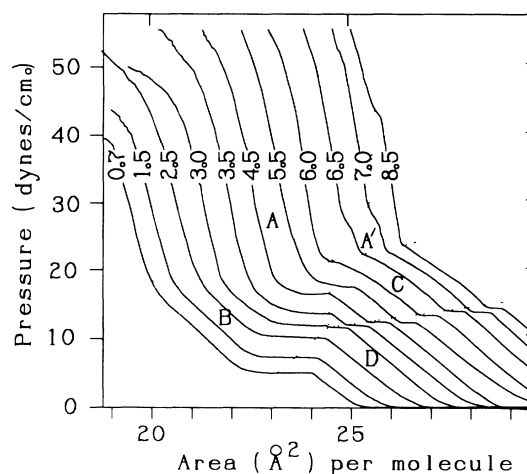


FIG. 1. Isotherms for monolayers of heneicosanoic acid on water (labels on isotherms indicate temperature in °C). The area axis labels are for the 0.7°C isotherm; other isotherms are shifted horizontally in multiples of 0.5 \AA^2 for clarity. The dotted lines are guides to the eye connecting similar features; the letters A–D are used to label regions for ease of reference.

measured on a $pH=2$ subphase (to further inhibit solubility) using the same trough used for x-ray studies. For $T \leq 2.5^\circ\text{C}$, the isotherms (Fig. 1) show a long plateau plus a rounded change of slope at a higher pressure; for $3^\circ\text{C} \leq T \leq 6^\circ\text{C}$, the single plateau splits into two shorter ones; and for $T \geq 6.5^\circ\text{C}$, each isotherm contains a plateau and a "kink" plus an irregular feature above the kink (we will show that this is also a phase transition). The dotted lines in Fig. 1 are guides to the eye connecting similar features; they divide the figure into five regions (labeled A , A' , B , C , and D for ease of reference). We have performed diffraction scans as a function of pressure at various temperatures; since the diffraction data are similar when the isotherms are similar, only data at $T=1.0^\circ\text{C}$, 5.0°C , and 8.0°C are discussed in this paper. Previous studies^{3,4} have established that these monolayers are powders in the plane; therefore, the trough was not turned during these experiments.

In region A , two first-order in-plane peaks are seen at 1.50 and 1.69 \AA^{-1} , so that this phase is solid (cf. Ref. 5); we will refer to these peaks as peak I and peak II. We recently reported¹¹ that we had seen two second-order peaks in this phase, and thus established that the

structure is distorted hexagonal (DH), i.e., face-centered orthorhombic. Of the three "bond lengths," two are 4.49 \AA and the third is 5.01 \AA ; thus peak I is doubly degenerate. A calculation based on in-plane peak intensities¹¹ (measured with a smaller vertical window than in the present experiments) shows that the molecules tilt slightly; however, these angles are small (usually $< 5^\circ$), and the vertical resolution used in the present work does not allow us to reliably distinguish such angles from zero. Therefore, for the purposes of this paper we will consider this phase as having vertical chains. (X-ray reflectivity studies^{12,13} also suggest that the molecules are vertical at high pressure, although of course this technique measures thickness and so is insensitive to small tilt angles.)

Figure 2 shows data in the pressure range covering regions A , A' , B , and C (i.e., excluding the low-pressure region D). The top row of panels shows segments of isotherms (note that pressure is now along the x axis). Throughout this pressure range, we see peak I and peak II; the magnitudes of the two diffraction vectors are shown in the next two rows of panels. Finally, $\tan^{-1}(k_z/k_{xy})$, i.e., the angle made by the diffraction vector relative to the horizontal, is shown in the lowest

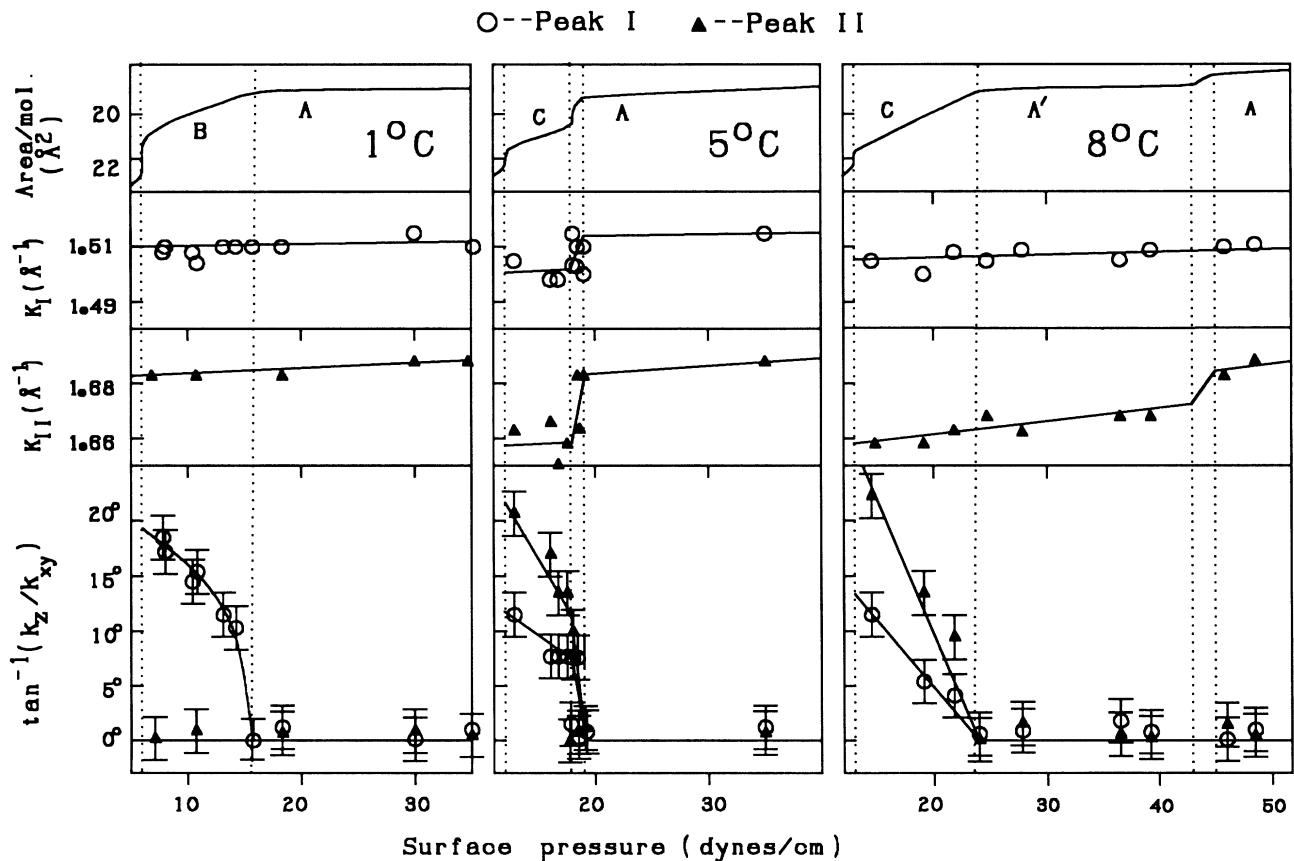


FIG. 2. Isotherms (top panels), diffraction vector magnitudes (center panels), and angles made by diffraction vectors relative to the horizontal (bottom panels), at three temperatures as labeled. Vertical dotted lines mark phase transitions (or, in cases of rounded transitions, the limits of the transition regions); solid lines through the data are guides to the eye.

row of panels. When the chains are vertical, these angles should be zero; nonzero angles indicate that the chains are tilted.

At 1°C (Fig. 2, left panels), it can be seen from the data that the chains are essentially vertical in the *A* phase; when the pressure is lowered and the monolayer enters the *B* phase, peak II remains in the plane but peak I moves continuously off the plane. The magnitudes K_I and K_{II} do not change noticeably at the transition. This establishes that the *B* phase consists of tilted molecules, and that the tilt direction is along the longer ($\sim 5 \text{ \AA}$) bond (see Fig. 3 for schematic: since the tilt direction is normal to \mathbf{K}_{II} , peak II remains unaffected while peak I moves off the plane). Thus the kink in the isotherm is a (solid-solid) tilting transition; it is not surprising that the onset of tilt causes a discontinuity in the compressibility but not in the density. Similar tilted-chain structures have previously been used as models to fit in-plane diffraction data from monolayers of various materials.^{8,11,14}

At 5°C, however, the peaks behave differently (Fig. 2, center panels). As the pressure is lowered from the *A* phase into the *C* region, not only do both peaks move off the plane, but peak II moves further from the plane than peak I. This means that we have a different tilted-chain structure: since peak I does not split, the tilt direction must be halfway between the two vectors corresponding to peak I and thus 90° away from the tilt direction in phase *B* (see Fig. 3 for schematic). Reasonably enough, the two tilt directions required to explain phases *B* and *C* are the two symmetry directions of the DH lattice. There is a jump in the diffraction-vector magnitudes, as well as in the magnitude of the tilt angle, at the *A-C* transition (which is a rounded flat section in the isotherm). In other words, a first-order change in the lattice structure has occurred simultaneously with the onset of tilt. (The bond lengths in the *C* phase are ~ 4.54 and

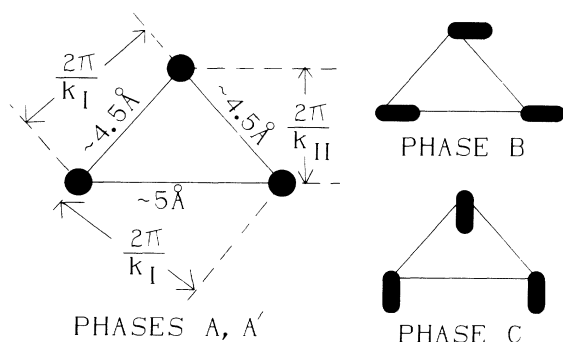


FIG. 3. Schematic showing the structures of the *A*, *A'*, *B*, and *C* phases. The *A* and *A'* structures are qualitatively the same, but the bond lengths differ slightly (see text). Solid objects represent projections of cylinders (schematically representing molecules) onto the horizontal plane, so that round indicates vertical and elongated indicates tilted.

$\sim 5.03 \text{ \AA}$.) We have observed a coexistence of in-plane and out-of-plane peaks in the transition region, which confirms that the transition is first order. The isotherm is rounded rather than flat in the coexistence region, but since there is no hydrodynamic equilibrium during a solid-solid transition, there is no reason for the isotherm to be absolutely flat.

At 8°C (Fig. 2, right panels), we see the same behavior within the *C* phase as at 5°C, but both x-ray data and isotherms are in agreement that the *C-A'* transition is continuous at 8°C. However, a first-order transition in the magnitude of K_{II} can be seen at the *A-A'* boundary. Although the change is small, it is larger than our resolution. K_I does not appear to change, but it is unlikely that it stays exactly constant; we assume that the change is too small to see (notice that $\Delta K_{II} > \Delta K_I$ at the *C-A* transition as well). The bond lengths in the *A'* phase are ~ 4.53 and $\sim 5.01 \text{ \AA}$. As before, we ascribe the nonideal shape of the isotherm to the lack of hydrodynamic equilibrium; in this case, both phases are very dense and presumably very rigid.

In region *D*, at low pressures, there is a resolution-limited in-plane peak at 1.44 \AA^{-1} , so that this phase is also solid. This is an unexpected result: the lowest-pressure segment of the isotherm is usually assumed to be fluid. Since the structure cannot be determined on the basis of one peak, we will refer to this phase only as an "expanded solid." At all temperatures, the 1.44-\AA^{-1} peak vanishes at the plateau marking the upper boundary of region *D*; we have seen peaks from the *B* and *D* phases simultaneously within the *B-D* transition region at 1°C.

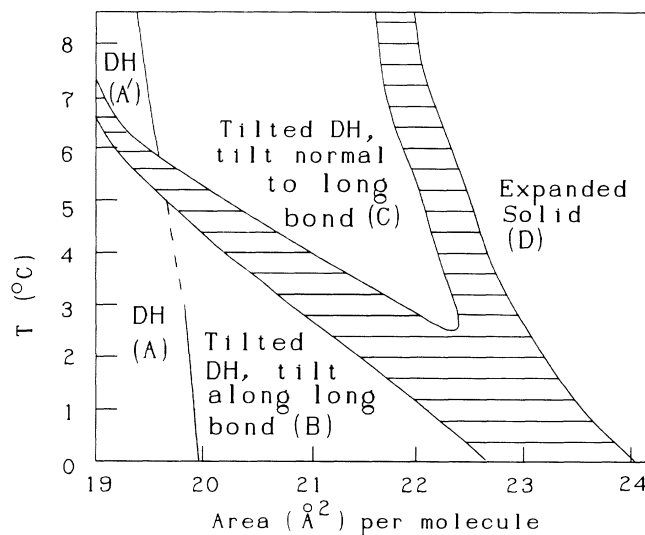


FIG. 4. Qualitative phase diagram (DH=distorted hexagonal). Striped areas are coexistence regions; the dashed line indicates a tentative (unverified) section of the phase boundary; the dotted lines indicate the temperatures for which data are shown in Fig. 2.

Our conclusions are summarized in Fig. 4. We see three lattice structures (two DH, and one expanded solid), and for the DH structures we identify tilted and untilted forms. Both isotherms and diffraction data show that transitions between different lattice structures are first order, while tilting transitions are continuous. We see no solid-fluid or fluid-fluid transitions in the temperature region studied. Although there is no reason to believe that these features are universal—fluid phases, for example, will presumably appear at sufficiently high temperatures or with other materials—our results discredit the practice of labeling phases liquid expanded, liquid condensed, etc., solely on the basis of isotherm shapes or other macroscopic evidence such as “viscosity” data. It should be noted that Ref. 8 identifies a zero-pressure solid even at room temperature in arachidic acid, a very similar material. Both Ref. 5 (studying heneicosanol) and Ref. 8 report an undistorted hexagonal room-temperature structure at high pressures; Ref. 5 describes a transition from undistorted to distorted along a high-pressure isobar as the temperature is lowered. Clearly, the phase diagrams of these systems are extremely rich and will reward further exploration, as a function of chain length, head group, subphase pH , etc.

We acknowledge extremely useful discussions with J. F. Nagle. This work was supported by the U.S. Department of Energy under Grant No. DE-FG02-84ER45125. The National Synchrotron Light Source (NSLS) and the Oak Ridge beam line (X-14) are also supported by the U.S. Department of Energy.

Note added.—We have recently determined that the expanded solid exists at zero pressure up to at least

60°C. Detailed studies are in progress.

¹See, e.g., G. L. Gaines, Jr., *Insoluble Monolayers at Liquid Gas Interfaces* (Interscience, New York, 1966).

²I. Langmuir, *J. Am. Chem. Soc.* **39**, 354 (1917).

³P. Dutta, J. B. Peng, B. Lin, J. B. Ketterson, M. Prakash, P. Georgopoulos, and S. Ehrlich, *Phys. Rev. Lett.* **58**, 2228 (1987).

⁴K. Kjaer, J. Als-Nielsen, C. A. Helm, L. A. Laxhuber, and H. Möhwald, *Phys. Rev. Lett.* **58**, 2224 (1987).

⁵S. Barton, B. Thomas, E. Flom, S. A. Rice, B. Lin, J. B. Peng, J. B. Ketterson, and P. Dutta, *J. Chem. Phys.* **89**, 2257 (1988).

⁶S. Grayer Wolf, M. Deutsch, E. M. Landau, M. Lahav, L. Leiserowitz, K. Kjaer, and J. Als-Nielsen, *Science* **242**, 1286 (1988).

⁷B. Lin, J. B. Peng, J. B. Ketterson, P. Dutta, B. Thomas, J. Buontempo, and S. A. Rice, *J. Chem. Phys.* **90**, 2393 (1989).

⁸K. Kjaer, J. Als-Nielsen, C. A. Helm, P. Tippman-Krayer, and H. Möhwald, *J. Phys. Chem.* **93**, 3200 (1989).

⁹See, e.g., W. D. Harkins and L. E. Copeland, *J. Chem. Phys.* **10**, 272 (1942).

¹⁰B. Lin, J. B. Peng, J. B. Ketterson, P. Dutta, B. N. Thomas, J. Buontempo, and Stuart A. Rice, *J. Chem. Phys.* **90**, 2393 (1989).

¹¹T. M. Bohanon, B. Lin, M. C. Shih, G. E. Ice, and P. Dutta, *Phys. Rev. B* **41**, 4846 (1990).

¹²M. J. Grundy, R. M. Richardson, S. J. Roser, J. Penfold, and R. C. Ward, *Thin Solid Films* **159**, 43 (1988).

¹³S. G. Wolf, E. M. Landau, M. Lahav, L. Leiserowitz, M. Deutsch, K. Kjaer, and J. Als-Nielsen, *Thin Solid Films* **159**, 29 (1988).

¹⁴S. Grayer-Wolf, M. Deutsch, E. M. Landau, M. Lahav, L. Leiserowitz, K. Kjaer, and J. Als-Nielsen, *Science* **242**, 1286 (1988).